Structure of the Vinyldiazomethyl Anion and Energetic Comparison to the Cyclic Isomers

Takatoshi Ichino, Adam J. Gianola, Shuji Kato, Veronica M. Bierbaum,* and W. Carl Lineberger*

JILA, University of Colorado and National Institute of Standards and Technology, and Department of Chemistry and Biochemistry, University of Colorado, Boulder, Colorado 80309-0440

Received: May 19, 2007; In Final Form: June 20, 2007

The 351.1 nm photoelectron spectrum of the vinyldiazomethyl anion has been measured. The ion is generated through the reaction of the allyl anion with N_2O in helium buffer gas in a flowing afterglow source. The spectrum exhibits the vibronic structure of the vinyldiazomethyl radical in its electronic ground state as well as in the first excited state. Electronic structure calculations have been performed for these molecules at the B3LYP/6-311++G(d,p) level of theory. A Franck−Condon simulation of the $\tilde{X}\ ^2A''$ state portion of the spectrum has been carried out using the geometries and normal modes of the anion and radical obtained from these calculations. The simulation unambiguously shows that the ions predominantly have an *E* conformation. The electron affinity (EA) of the radical has been determined to be 1.864 ± 0.007 eV. Vibrational frequencies of 185 ± 10 and 415 ± 20 cm^{-1} observed in the spectrum have been identified as in-plane CCN bending and CCC bending modes, respectively, for the $\tilde{X}\ ^2A''$ state. The spectrum for the $\tilde{A}\ ^2A'$ state is broad and structureless, reflecting large geometry differences between the anion and the radical, particularly in the CCN angle, as well as vibronic coupling with the $\tilde{X}\ ^2A''$ state. The DFT calculations have also been used to better understand the mechanism of the allyl anion reaction with N_2O. Collision-induced dissociation of the structural isomer of the vinyldiazomethyl anion, the 1-pyrazolide ion, has been examined, and energetics of the structural isomers is discussed.

Introduction

We have recently studied the thermodynamic properties of nitrogen-containing, five-membered compounds, pyrrole,[1] imidazole,[2] and pyrazole,[3] to better understand the effects of N atoms on these properties. These studies are motivated by interest in nitrogen-rich compounds as possible high energy-density materials.[4−10] In the reaction of the hydroxide ion (HO^-) with imidazole, we find that HO^- is sufficiently basic that a proton can be abstracted not just from the N−H site, the most exothermic reaction pathway, but also from the C5 position of imidazole.[2] Thus, the reaction produces two structural isomers of the imidazolide ion, i.e., 1-imidazolide and 5-imidazolide. The same observation has been made for the HO^- reaction with pyrazole.[3] These findings allow us to discuss the structural dependence of the ion energetics and the effects of the N atoms on the energetics.

These structural isomers maintain the five-membered cyclic form. Another question involves how the energetics changes when this cyclic structure is ruptured. In the present study, we address this issue in the case where two N atoms are contained in the ring.

The reactivity of carbanions toward nitrous oxide (N_2O) in the gas phase has been studied by DePuy and co-workers.[11−13] Bierbaum et al. have found that the reaction of the allyl anion with N_2O leads to formation of the vinyldiazomethyl anion.[11]

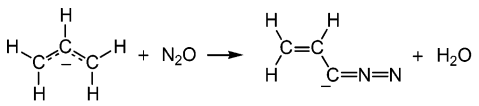

(1)

This and subsequent investigations have determined the rate coefficient of the reaction, the minor reaction products, and the branching ratios at room temperature.[11−13] The vinyldiazomethyl anion is a structural isomer of the pyrazolide and imidazolide ions (Figure 1). Its reactivities with carbon dioxide (CO_2), carbonyl sulfide (COS), and carbon disulfide (CS_2) have been studied,[14] but the structure and energetics of the vinyldiazomethyl anion are not well-known.

In this article, we report the photoelectron spectrum of the vinyldiazomethyl anion. Electronic structure calculations on the ion and the neutral radical generated through photodetachment, the vinyldiazomethyl radical, have been performed at the B3LYP/6-311++G(d,p) level of density functional theory (DFT). Spectral simulations have been attempted using the results of the DFT calculations. The observed spectrum has been well reproduced, and the simulation unambiguously indicates that the ions produced in the flow tube are predominantly *E*-conformers. The mechanism of the reaction of the allyl anion with N_2O has been studied through DFT calculations. CID of the 1-pyrazolide and 1-imidazolide ions has also been carried out to address the stability of these ions. The energetics of the vinyldiazomethyl anion will be discussed in comparison with these stable structural isomers.

Experimental Section

The ultraviolet anion photoelectron spectrometer has been described in detail elsewhere.[15−17] A microwave discharge of helium buffer gas (~0.4 Torr) containing a small amount of oxygen (O_2) produces atomic oxygen ion (O^-) in the flowing afterglow ion source. A trace amount of propene is added downstream in the flow tube, reacting rapidly with O^- to form HO^-. HO^- reacts with propene to form the allyl anion ($C_3H_5^-$).[18] A trace amount of N_2O is added further downstream

* Corresponding authors: wcl@jila.colorado.edu, veronica.bierbaum@colorado.edu.

10.1021/jp073887v CCC: $37.00
Published on Web 08/04/2007

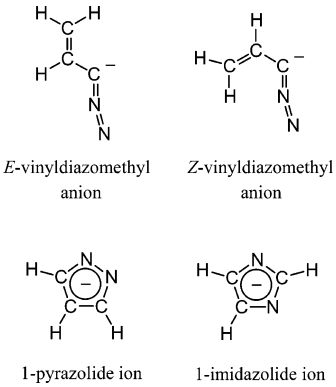

Figure 1. Structure of the vinyldiazomethyl anion, 1-pyrazolide, and 1-imidazolide ions.

to convert $C_3H_5^-$ to the vinyldiazomethyl anion ($C_3H_3N_2^-$).[11] These reactions take place in a flow tube at room temperature, or in a flow tube cooled by a flow of liquid nitrogen such that the ion temperature can be decreased below room temperature through collisions with the cold helium buffer gas. The anions are extracted from the flow tube into a differentially pumped region, accelerated to 735 eV, and focused into a Wien velocity filter for mass selection. The mass-selected ion beam is refocused, decelerated to 35 eV, and overlapped with a laser beam in a high-vacuum build-up cavity to photodetach electrons. The output of a continuous wave (CW) argon ion laser (351.1 nm, 3.531 eV) is amplified in the cavity with a circulating power up to 100 W. A typical beam current is 100 pA for the vinyldiazomethyl anion.

Photodetached electrons emitted into a small solid angle perpendicular to both the ion and laser beams are collected and focused into a hemispherical energy analyzer with a kinetic energy resolution of 8−10 meV. The energy analyzed photoelectrons are magnified onto the microchannel plates for amplification and imaged onto the position sensitive detector. Photoelectron spectra are recorded as the electron kinetic energy (eKE) of the analyzer is scanned. The spectra are presented as a function of electron binding energy (eBE), which is equal to the difference between the laser photon energy (3.531 eV) and eKE. The absolute kinetic energy is calibrated by measuring the photoelectron spectrum of O^-, an ion for which the electron binding energy is very accurately known.[19,20] A small (<1%) energy scale compression factor[15] is taken into account by measuring the photoelectron spectrum of W^-, and utilizing the well-known term energies of the excited states of the W atom.[21] A rotatable half-wave plate is inserted into the laser beam path before the build-up cavity to control the angle (θ) between the electric field vector of the laser beam and the photoelectron momentum vector. The intensity of the photoelectrons depends on θ according to[22]

$$I(\theta) = \frac{\sigma_o}{4\pi}(1 + \beta P_2(\cos\theta)) \qquad (2)$$

where σ_0 is the total photodetachment cross section, β is the anisotropy parameter, and $P_2(\cos\theta)$ is the second Legendre polynomial. Measurements at the magic angle (54.7°) provide spectra free from the angular dependence. The β value is determined by measuring the relative photodetachment cross section at several values of the collection angle, θ, and fitting the data to the form in eq 2.

Collision-induced dissociation (CID) of the pyrazolide and imidazolide ions has been studied using a tandem flowing afterglow-selected ion flow tube (FA-SIFT) instrument.[23,24]

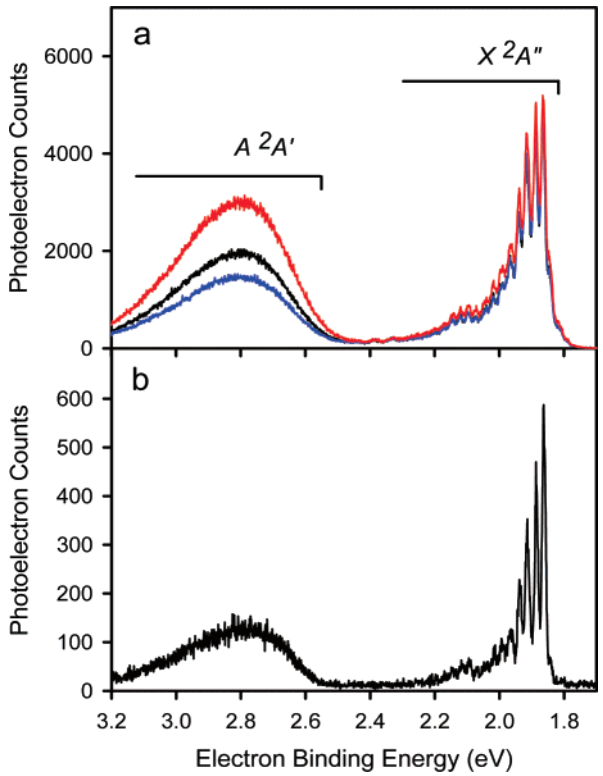

Figure 2. Photoelectron spectra (351.1 nm) of the vinyldiazomethyl anion. The ions were synthesized in a flow tube at room temperature (a) and in a flow tube cooled with liquid nitrogen (b). The θ values are 54.7° (black), 0° (red), and 90° (blue).

These ions were synthesized in the source flow tube through the reaction of HO^- with pyrazole and imidazole. Following mass-selection with a SIFT quadrupole mass filter, the ions were injected into the second flow tube containing helium (~0.5 Torr) at different injection energies (10−80 eV lab energy). CID takes place upon collision of the ion with the helium buffer gas in the vicinity of the injection orifice. Multiple collisions can occur during excitation and dissociation of the ion under the experimental conditions. The reactant and product ions were analyzed using a detection quadrupole mass filter at the end of the second flow tube. By measuring CID of CF_3^- and CCl_3^- and comparing the results with those reported in the literature,[25] CID threshold energies determined experimentally were semiquantitatively calibrated to those corresponding to single-collision conditions.

All the electronic structure calculations were performed at B3LYP/ 6-311++G(d,p) level[26−28] using the Gaussian 03 program package.[29] The thermodynamic quantities evaluated with the DFT calculations are reported with zero-point energy corrections taken into account under the harmonic assumption. Harmonic frequencies were used without scaling.

Results and Discussion

A. Photoelectron Spectrum of the Vinyldiazomethyl Anion. The 351.1 nm photoelectron spectra of the vinyldiazomethyl anion are shown in Figure 2a. The ions were synthesized in a flow tube at room temperature. The spectra were taken at $\theta = 0°$, 54.7°, and 90°. The observed spectrum consists of two parts. In the region of electron binding energies (eBE) between 1.8 and 2.3 eV, relatively well-resolved vibronic peaks are present. However, in the region of eBE above 2.5 eV, the spectral profile is broad and structureless. The intensity of this second portion of the spectrum is considerably enhanced relative to that of the lower eBE portion for $\theta = 0°$, and suppressed for

TABLE 1. B3LYP/6-311++G(d,p) Optimized Geometries for *E*-Vinyldiazomethyl Anion, *E*-Vinyldiazomethyl Radical, *Z*-Vinyldiazomethyl Anion, and *Z*-Vinyldiazomethyl Radical[a]

	E-anion	*E*-radical		*Z*-anion	*Z*-radical
	$\tilde{X}\ ^1A'$	$\tilde{X}\ ^2A''$	$\tilde{A}\ ^2A'$	$\tilde{X}\ ^1A'$	$\tilde{X}\ ^2A''$
NN	1.1690	1.1507	1.1903	1.1671	1.1503
NC_α	1.2654	1.2815	1.2072	1.2670	1.2803
$C_\alpha C_\beta$	1.4243	1.4184	1.3987	1.4298	1.4205
$C_\beta C_\chi$	1.3629	1.3586	1.3459	1.3668	1.3609
$C_\beta H$	1.1009	1.0906	1.0902	1.0925	1.0853
$C_\chi H_\alpha$	1.0853	1.0834	1.0812	1.0864	1.0839
$C_\chi H_b$	1.0858	1.0836	1.0823	1.0861	1.0848
$\angle NNC_\alpha$	173.23	170.02	178.68	173.15	169.88
$\angle NC_\alpha C_\beta$	121.14	122.34	173.01	121.95	123.84
$\angle C_\alpha C_\beta C_\chi$	127.42	121.15	127.24	130.16	126.01
$\angle C_\alpha C_\beta H$	116.86	119.94	113.35	114.10	115.32
$\angle C_\beta C_\chi H_a$	121.01	121.27	119.85	120.86	121.01
$\angle C_\beta C_\chi H_b$	121.22	120.58	122.24	121.91	121.78

[a] Bond lengths are in units of angstroms, and bond angles are in units of degrees. See Figure 1 for the drawings of the molecular structures. In both conformers, $C_\alpha C_\beta C_\chi H_a$ dihedral angle is 180° while $C_\alpha C_\beta C_\chi H_b$ dihedral angle is 0°.

$\theta = 90°$. The β values are determined to be 0.50 ± 0.10 and 0.10 ± 0.10 for the higher and lower eBE portions of the spectrum, respectively. The distinct angular dependence of the photodetachment efficiency strongly suggests that the two portions represent different electronic states of the vinyldiazomethyl radical, with electron photodetachment coming from two different orbitals of the anion.

It is relevant at this point to recall the photoelectron spectroscopic study of the diazomethyl anion.[30] The photoelectron spectrum exhibited transitions to both the electronic ground state ($\tilde{X}^2A''$) and the first excited state ($\tilde{A}\ ^2A'$) of the diazomethyl radical, with the $\tilde{X}\ ^2A''$ portion of the spectrum characterized by a sharp, intense origin peak accompanied by a few, very small, resolved vibrational peaks; the $\tilde{A}\ ^2A'$ portion of the spectrum was quite broad with some vibrational peaks superimposed. The β values are -0.8 and 0.0 for the $\tilde{X}\ ^2A''$ and $\tilde{A}\ ^2A'$ states, respectively, a trend analogous to that seen for the vinyldiazomethyl anion. Thus, it is most likely that the two portions of the spectrum in Figure 2 represent the ground and first excited states of the vinyldiazomethyl radical.

To further analyze the spectrum, we have carried out electronic structure calculations at the B3LYP/6-311++(d,p) level of theory. Table 1 summarizes the optimized geometries of the ground state of the *E*-vinyldiazomethyl anion and the ground and first excited states of the *E*-vinyldiazomethyl radical. All the stationary points were located with C_s symmetry. Harmonic frequency analysis shows that the potential energy surfaces of the ground states of both the anion and the neutral radical have minima at the corresponding optimized geometries, while the excited-state of the radical is a transition state with an imaginary frequency for the out-of-plane CCN bending mode. The calculations predict the electron affinity (EA) of the *E*-vinyldiazomethyl radical to be 1.869 eV and the term energy of the first excited-state to be 0.496 eV. The calculated EA value matches the eBE for the most intense peak in the lower eBE portion of the spectrum in Figure 2, while the energy separation between the intense peak and the onset of the broad feature observed in the higher eBE portion of the spectrum is significantly larger than the calculated term energy for the first excited state.

B. Spectral Simulation. We have attempted to simulate the spectrum for the radical ground state based on the results of the DFT calculations of the optimized geometries and harmonic frequency analysis for the ground states of the anion and the radical, using the *PESCAL* program.[31,32] Simulations were performed for the photoelectron spectrum of the vinyldiazomethyl anion produced in a flow tube cooled with liquid nitrogen. Figure 2b shows the spectrum taken under such conditions. The cooling reduces the vibrational (as well as rotational) temperature of the ions, which results in diminished contributions from vibrationally excited ions to the photoelectron spectrum. Consequently, the observed spectrum is better resolved. The simulation provides the relative intensities of individual vibronic transitions, which are displayed as sticks in Figure 3a. These transitions were convoluted with a Gaussian function with a full-width at half-maximum of 14 meV. The solid line in Figure 3a represents the simulated spectrum, while the observed spectrum is shown as dots. A vibrational temperature of 150 K

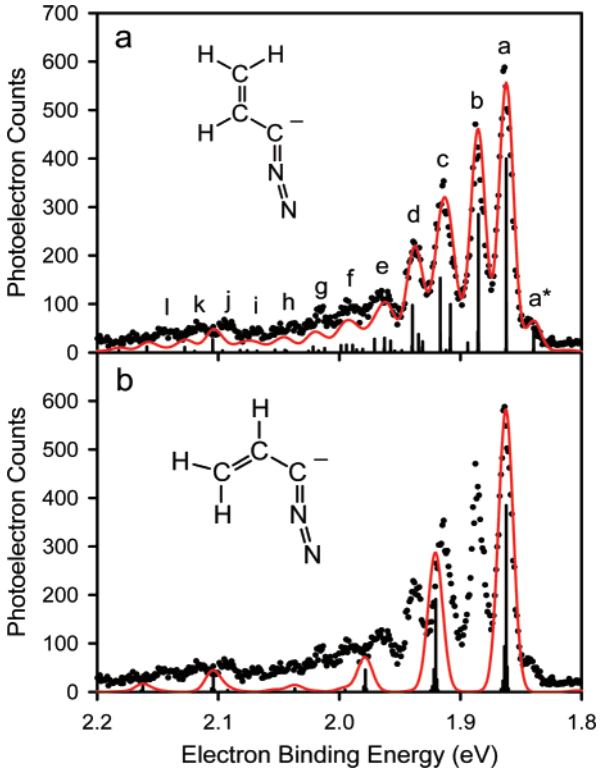

Figure 3. Simulations of the photoelectron spectrum of the vinyldiazomethyl anion. Sticks represent relative positions and intensities of vibronic transitions from the $\tilde{X}\ ^1A'$ *E*-vinyldiazomethyl anion (a) and *Z*-vinyldiazomethyl anion (b) to the $\tilde{X}\ ^2A''$ states of the corresponding radicals. The solid lines are Gaussian convolutions of the transitions with a full width at half-maximum of 14 meV. A vibrational temperature of 150 K was assumed for the anions in the simulations. Dots are the experimental data, shown in Figure 2b, obtained at the magic angle.

TABLE 2. Peak Positions and Assignments for the Photoelectron Spectrum of *E*-Vinyldiazomethyl Anion

peak[a]	peak position (cm^{-1})[b]	assignment[c]
a*	-160 ± 15	13_1^0
a	0	0_0^0
b	185 ± 10	13_0^1
c	405 ± 15	12_0^1 and 13_0^2
d	605 ± 15	$12_0^1\,13_0^1$ and 11_0^1
e	810 ± 40	
f	1035 ± 70	
g	1240 ± 35	
h	1425 ± 30	
i	1660 ± 35	
j	1860 ± 30	4_0^1
k	2045 ± 25	
l	2250 ± 35	

[a] Peak labels used in Figure 3a. [b] Relative to the origin peak (peak a). [c] The ν_4 mode is the NNC asymmetric stretching, ν_{11} is the NNC bending, ν_{12} is the CCC bending, and ν_{13} is the NCC bending modes. All these modes are in-plane (a') modes.

was assumed for the anion in the simulation. The simulated origin peak is set to match the position and intensity of the observed peak a in Figure 3a. The simulation reproduces the observed spectrum very well. Thus, peak a represents the 0−0 transition from the vibrational ground level of $\tilde{X}\ ^1A'$ *E*-vinyldiazomethyl anion to that of $\tilde{X}\ ^2A''$ *E*-vinyldiazomethyl radical, and the EA of the *E*-vinyldiazomethyl radical is determined to be 1.864 ± 0.007 eV. The DFT-calculated value, 1.869 eV, is in good agreement with the experimental value. The Franck−Condon simulation also helps identify the vibrational peaks. Peak b represents the fundamental level of the in-plane CCN bending mode of the $\tilde{X}\ ^2A''$ radical with a frequency of 185 ± 10 cm^{-1}. There are two vibronic transitions largely contributing to peak c. One is the fundamental level of the in-plane CCC bending mode, and the other is the overtone level of the CCN bending mode. The energy separation of the two transitions is not sufficiently large to be resolved in our measurements. The peak position relative to peak a is 405 ± 15 cm^{-1}, but the fundamental vibrational frequency of the CCC bending mode may be slightly higher than this value. Peak d (605 ± 15 cm^{-1}) is primarily composed of a combination of the CCN bending and CCC bending modes. From the positions of peaks b, c, and d, the fundamental vibrational frequency of the CCC bending mode of the $\tilde{X}\ ^2A''$ radical is determined to be 415 ± 20 cm^{-1}. Also, peak j likely represents the fundamental level of the asymmetric CNN stretching mode with a frequency of 1860 ± 30 cm^{-1}. Peak a*, located to the lower eBE side of peak a, is a hot band transition from a vibrationally excited level of the anion to the vibrational ground level of the radical. The simulation indicates that it corresponds to the excitation of the in-plane CCN bending mode of the anion, and its fundamental vibrational frequency is determined to be 160 ± 15 cm^{-1}. The observed peak positions and their assignments are summarized in Table 2. The lower panel b in Figure 3 is a simulation for a different conformer of the vinyldiazomethyl anion, as discussed extensively in Section C.

In contrast to the $\tilde{X}\ ^2A''$ state portion of the spectrum, the higher eBE portion of the spectrum is broad and structureless (Figure 2). Comparison to the photoelectron spectrum of the diazomethyl anion[30] suggests that photodetachment to $\tilde{A}\ ^2A'$ *E*-vinyldiazomethyl radical accounts for this portion of the spectrum, and we present arguments below to support this conclusion.

The onset of the broad feature of the spectrum occurs about 0.7 eV above the origin of the $\tilde{X}\ ^2A''$ state. While this separation is significantly larger than the DFT evaluated term energy of ~0.5 eV, it is consistent with the considerable geometry difference between the $\tilde{X}\ ^1A'$ anion and the $\tilde{A}\ ^2A'$ radical. Table 1 shows that the CCN angle is 121.14° for the anion, but it is 173.01° for the $\tilde{A}\ ^2A'$ radical. Such a large geometry change makes it certain that Franck−Condon overlap between the initial anion nuclear wave function and the nuclear wave function for the vibrational ground level of the $\tilde{A}\ ^2A'$ radical is negligibly small. Such observations have been made for the photodetachment from, for example, the coinage metal trimer anions[33] and CuH_2^-.[34] Consequently, relatively large Franck−Condon overlap is possible only for highly vibrationally excited levels of the $\tilde{A}\ ^2A'$ radical. Indeed, the potential energy of the $\tilde{A}\ ^2A'$ radical at the anion geometry is calculated to be 0.45 eV higher than that at its stationary point geometry shown in Table 1. In other words, the DFT calculations evaluate the vertical detachment energy to be 2.816 eV. The maximum of the broad feature of the spectrum in Figure 2 is located around an eBE of 2.8 eV. Thus, the DFT calculations support the conclusion that the broad spectral profile represents the $\tilde{A}\ ^2A'$ radical.

Our DFT calculations indicate that the harmonic vibrational frequency for the in-plane CCN bending mode of the $\tilde{A}\ ^2A'$ radical is 96 cm^{-1}. The shallow potential energy well along this coordinate together with possible significant anharmonicity and contributions from the other modes might also provide an explanation for the structureless broad profile of the spectrum. Another important aspect is the vibronic coupling between the $\tilde{X}\ ^2A''$ and $\tilde{A}\ ^2A'$ states. It is again relevant to refer to the unsubstituted diazomethyl system.[30] The $\tilde{X}\ ^2A''$ and $\tilde{A}\ ^2A'$ states of the diazomethyl radical form a Renner−Teller pair; they are degenerate at the linear geometry. In the case of the vinyldiazomethyl radical, the vinyl group prevents symmetrically enforced degeneracy. However, the DFT calculations predict that the potential energy of the $\tilde{X}\ ^2A''$ state is only 53 meV below that of the $\tilde{A}\ ^2A'$ state at the equilibrium geometry of the $\tilde{A}\ ^2A'$ state. Along the out-of-plane coordinates these two states can be coupled with each other, and consequently there are many vibronic levels contributing to the $\tilde{A}\ ^2A'$ state portion of the spectrum.[35] Such an effect certainly can broaden the spectrum, as observed, for example, in the photoelectron spectrum of pyrrole.[36]

C. Conformation of the Vinyldiazomethyl Anion. In the preceding section, the vibronic feature observed in the $\tilde{X}\ ^2A''$ state portion of the spectrum is well explained through the Franck−Condon simulation. It should be noted, however, that the vinyldiazomethyl anion can also assume a *Z* conformation with respect to the CCCN nuclear configuration (Figure 1). Indeed, our DFT calculations find a local minimum for the *Z* conformer. The calculations predict that the *Z* conformer lies 2.1 kcal mol^{-1} higher in energy than the *E* conformer. It is not clear how accurately the DFT calculations can provide energetic information. Some fraction of the ions synthesized in the flow tube might have the *Z* conformation. DFT calculations were also performed for the *Z*-vinyldiazomethyl radical. The EA of the *Z*-radical is evaluated to be 1.873 eV. This value is also very close to the eBE of peak a (Figure 3a).

We have found that the spectral simulation can give a definitive answer to this question. Figure 3b shows the results of the simulation for the transition from $\tilde{X}\ ^1A'$ *Z*-vinyldiazomethyl anion to $\tilde{X}\ ^2A''$ *Z*-vinyldiazomethyl radical. Clearly, the spectral simulation fails to reproduce the observed vibronic features. Comparison of the simulations for the *E* and *Z*

conformers shown in Figures 3a and 3b unambiguously indicates that the vinyldiazomethyl anions produced in the flow tube are predominantly *E* conformers.

The two conformers can be converted to each other through rotation around the $C_\alpha C_\beta$ bond (Figure 1). The transition state has been located for this conversion process in the DFT calculations, and it is 5.9 kcal mol^{-1} higher in energy adiabatically than the *Z*-anion ground state. If thermal equilibration is achieved at 150 K, then the population of the *Z*-anion would be about 0.1% according to the energetics predicted by the DFT calculations. Thus, the energetic information obtained from the DFT calculations is at least consistent with the conclusion, drawn from the spectral simulation, that the ions are predominantly *E* conformers. It should be noted that B3LYP/6-31+G-(d) calculations provide energetics of conformers of *o*- and *m*-ethynylstyrene that is consistent with results of a spectroscopic study by Zwier and co-workers.[37]

Comments on the difference in the Franck−Condon overlap between the two conformers displayed in Figure 3 will be given here. The simulated spectrum for the *Z*-anion is characterized by a vibrational progression for the in-plane CCC bending mode. This mode is also active in the simulated spectrum for the *E*-anion. However, the low frequency in-plane CCN bending mode is active in the *E*-anion spectrum but not in the *Z*-anion spectrum. The DFT calculations yield harmonic frequencies of 186 and 158 cm^{-1} for the CCN bending mode of the *E*-radical and *Z*-radical, respectively.

Generally, activation of a vibrational mode upon electronic transition results from a significant geometrical difference between the initial and final states along the normal coordinate. This explanation is appropriate for the CCC bending coordinate. Photodetachment from the *E*-anion brings about a decrease in the CCC angle from 127.42° to 121.15° according to the DFT calculations (Table 1). The corresponding change for the *Z* conformers is from 130.16° to 126.01°. The significant changes in the bond angle results in the appearance of the vibrational peaks for the CCC bending mode in the simulations of both conformers.

The similar arguments, however, seemingly fail to explain the difference in the simulations of the two conformers with respect to the CCN bending mode. The DFT calculations predict that the CCN angle changes from 121.14° (anion) to 122.34° (radical) for the *E* conformers, while the corresponding change for the *Z* conformers is from 121.95° to 123.84° (Table 1). The magnitude of the bond angle change is small and comparable for the two systems, or it is larger for the *Z* conformers, but the vibrational peaks for the CCN bending mode appear only in the *E* conformer simulation.

This discussion is oversimplified, however, since what really matter are the normal coordinate displacements involving all of the nuclei.[38] Our calculations show that the magnitude of such displacement is 1.150 for the *E* conformer and 0.054 for the *Z* conformer, along the CCN bending normal coordinate in dimensionless units. This difference in the magnitude of the displacement results in distinct spectral simulations as shown in Figure 3.

This difference can be understood qualitatively as follows. For the transitions from $\tilde{X}\ ^1A'$ *E*-vinyldiazomethyl anion to $\tilde{X}\ ^2A''$ *E*-vinyldiazomethyl radical, the geometry changes involve a decrease in the CCC angle, an increase in the CCN angle, and a decrease in the CNN angle (see Table 1 as well as discussion given above). Displacement along the CCN bending normal coordinate inevitably translates the terminal C atom (as well as the attached H atoms) and N atom significantly. The geometry changes induced by photodetachment from the *E* anion are in phase with the overall nuclear displacements along the CCN bending coordinate. Therefore, the vibrational peaks for the CCN bending mode are relatively active in the simulation, as shown in Figure 3a. On the other hand, in the case of the *Z* conformers, the geometry shifts of the terminal C and N atoms for the detachment process are in opposite directions, so that they are out of phase with the overall nuclear displacements along the CCN bending coordinate. Instead, the CCC bending mode, coupled with the CNN bending mode, is totally in phase with the geometry shifts, which manifests itself in the simulation in Figure 3b.

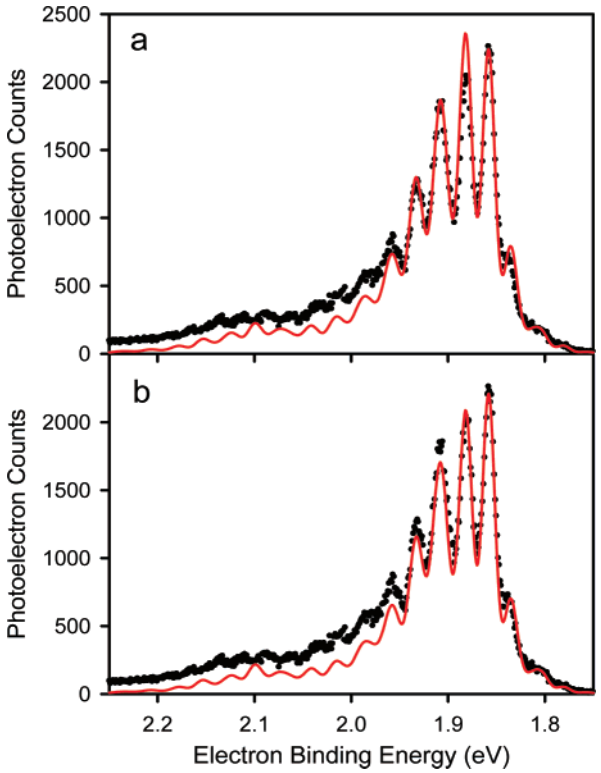

Figure 4. Simulations of the photoelectron spectrum of the vinyldiazomethyl anion shown as solid lines. A vibrational temperature of 300 K was assumed in the simulations. The simulations represent detachment from the $\tilde{X}\ ^1A'$ *E*-vinyldiazomethyl anion exclusively (a) and from both *E*- and *Z*-vinyldiazomethyl anions with 0.962:0.038 population ratio (b) to the $\tilde{X}\ ^2A''$ states of the corresponding radicals. Dots are the experimental data, shown in Figure 2a, obtained at the magic angle.

Franck−Condon simulations have also been performed for the spectrum of the vinyldiazomethyl anion synthesized in the flow tube at room temperature. The vibrational temperature of the anion is assumed to be 300 K in the simulations. Figure 4a shows the results of the simulation for the *E*-vinyldiazomethyl anion. As before, the simulated spectrum is set to match the observed origin peak a. The quality of the fit is good, but some discrepancy in the relative intensities of peaks a and b is noticeable. According to the DFT calculations, the free energy difference between the two conformers is 1.9 kcal mol^{-1} at 300 K, corresponding to an equilibrium population ratio of 0.962: 0.038 for the *E*- and *Z*-conformers. Figure 4b displays the results of the simulation with both conformers taken into account with this ratio. The transition dipole moments for the detachment from the two anions were assumed to be identical. It was also assumed that the EAs of the *E*- and *Z*-radicals are the same. The relative intensity of peak b is somewhat reduced in the simulation, and the simulated spectrum in Figure 4b appears to better fit the observed spectrum than does the simulation in

Figure 4a. Therefore, the spectrum of the anion produced at room temperature may contain nonnegligible contributions from the *Z*-vinyldiazomethyl anion.

The present work clearly demonstrates that the Franck−Condon profiles of the photoelectron spectra can provide useful experimental information for insight into conformations of organic molecules. It should be mentioned that recent advancements in high-resolution gas-phase spectroscopic techniques have prompted a number of experimental studies addressing conformational structure of neutral organic molecules.[37,39−47] There are also a few experimental studies directly exploring chemistry specific to conformational isomers of anions in the gas phase. Squires and co-workers studied reduction of cyclic ketones by pentacoordinate silicon hydride ions.[48,49] They explored the diastereoselectivity of the reactions through CID of the reaction product ions. They have also found a significant difference in the gas-phase acidity between the diastereoisomers of 2-*tert*-butyl-1,3-dithian-5-ol.[50] A conformational dependence of ion energetics was also the main issue in an experimental study of the gas-phase acidities of lactones by Brauman and co-workers.[51] Chou and Kass stereospecifically synthesized 1-propenyl ions and studied their reactivity toward N_2O.[52] They found quite different distributions of the product ions between the *E* and *Z* conformers.

Roemer and Brauman synthesized the propionaldehyde enolate ions stereospecifically and measured their photodetachment spectra.[53] They concluded that the EAs of the *E*- and *Z*-enolate radicals are 1.619 ± 0.007 and 1.73 ± 0.01 eV, respectively, based on the threshold behaviors. Their experimental approach is qualitatively different from ours in that they know the ion structure beforehand because of the synthesis method. This technique would not be effective for identification of the stereoisomers in cases where the electron binding energies are very similar. The EAs of the two conformers of the vinyldiazomethyl radical evaluated by the DFT calculations differ only by 4 meV.

Vibronic profiles of the photoelectron spectra are more informative with respect to identification of conformational structures, as described in this article. Indeed, Continetti and co-workers adopted the same approach in their study of the propionaldehyde enolate ions.[54] They generated the ions by seeding a mixture of N_2O and propanol in Ar in a pulsed discharge ion source. Thus, they did not know a priori the conformation(s) in which the ions were synthesized. They determined the ratio of the two conformers from the spectral simulations. However, the quality of the spectral fitting was only fair. Two issues might have compromised their spectral analysis. One is that the level of the electronic structure calculations employed in their study, CASSCF/6-311++G(d,p), may not be adequate for the spectral simulations. The other issue is that their spectrometer has a limited energy resolution that, together with some uncertainty of the vibrational temperature of the ions, makes it difficult to achieve accurate spectral simulations. The present work is free from these minor problems. The ions are cooled in the flow tube, the vibronic peaks are well resolved, and the quality of the spectral simulation is excellent.

D. Electronic Structure of the Vinyldiazomethyl Anion. The EA of the *E*-vinyldiazomethyl radical, 1.864 ± 0.007 eV, is larger than that of the unsubstituted diazomethyl radical,[30] 1.685 ± 0.006 eV, by 0.18 eV. Since electron photodetachment to the $\tilde{X}\ ^2A''$ state removes an electron from the π molecular orbital of the ion, it seems that there is significant delocalization of the π molecular orbital. While there is minimal vibrational activity observed in the photoelectron spectrum for $\tilde{X}\ ^2A''$ diazomethyl radical, the photoelectron spectrum for $\tilde{X}\ ^2A''$ *E*-vinyldiazomethyl radical exhibits prominent vibrational peaks principally associated with the in-plane CCN and CCC bending modes. A modest vibrational progression along the CCC bending mode has been observed in the photoelectron spectrum of the allyl anion.[18] The fundamental vibrational frequency of the CCC bending mode of $\tilde{X}\ ^2A''$ *E*-vinyldiazomethyl radical, 415 ± 20 cm^{-1}, determined in the present study, is very close to that for the allyl radical, 425 ± 10 cm^{-1}.[18] The progression of the CCC bending mode for the vinyldiazomethyl radical spectrum, however, is not as extensive as that observed in the allyl radical spectrum. The small vibrational peaks observed in the photoelectron spectrum of the diazomethyl anion represent the in-plane CNN bending and CNN asymmetric stretching modes of the diazomethyl radical.[30] As discussed earlier, peak j in Figure 3a corresponds to the CNN asymmetric stretching mode of $\tilde{X}\ ^2A''$ *E*-vinyldiazomethyl radical. Our Franck−Condon overlap calculations reveal a small intensity for the transition to the fundamental level of the CNN bending mode as well, but it is overwhelmed by the transition to the combination level of the in-plane CCN bending and CCC bending modes, which mainly accounts for peak d (Figure 3a).

The π electron delocalization can also be recognized from the assessment of the stabilization energy due to the vinyl group for the diazomethyl anion. McAllister and Tidwell used the following isodesmic reaction and calculated the stabilization energy for the vinyldiazomethane to be 1.4 kcal mol^{-1} at the MP2/6-31G(d) level.[55,56]

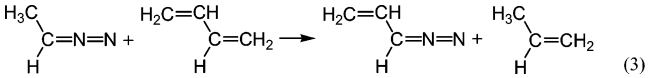

(3)

A similar reaction can be set up for the corresponding anion.

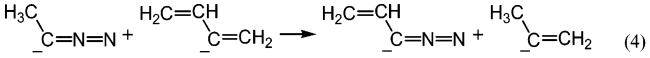

(4)

We estimate the stabilization energy for the *E*-vinyldiazomethyl anion to be 7.6 kcal mol^{-1} at the B3LYP/6-311++G(d,p) level.[57]

When the DFT geometry of the *E*-vinyldiazomethyl anion is compared with that of the diazomethyl anion, we find minimal differences in the bond lengths of the diazomethyl group between the vinyl-substituted and unsubstituted anions. The calculated CN and NN bond lengths are 1.2654 and 1.1690 Å, respectively, for the *E*-vinyldiazomethyl anion (Table 1), while the corresponding values for the diazomethyl anion are 1.2672 and 1.1758 Å. The CC bond length of the vinyl group is calculated to be 1.3629 Å, but the $C_\alpha C_\beta$ bond length is 1.4243 Å for the *E*-vinyldiazomethyl anion. The CC bond length for the allyl anion is calculated to be 1.3942 Å. These considerations indicate that there is only modest delocalization over the vinyl group in the vinyldiazomethyl anion.

E. Energetics of the Vinyldiazomethyl Anion and Its Structural Isomers. In solution, vinyldiazomethane thermally cyclizes to form 3*H*-pyrazole followed by tautomerization to 1*H*-pyrazole.[58,59] The cyclization requires an out-of-plane rotation of the vinyl group, with a substantial energy barrier for the process. An activation energy for the cyclization has been experimentally determined to be 22.6 kcal mol^{-1},[60] which electronic structure calculations predict very well.[61] The cyclization process itself is calculated to be about 5 kcal mol^{-1} exothermic,[61] but the overall exothermicity from vinyldiaz-

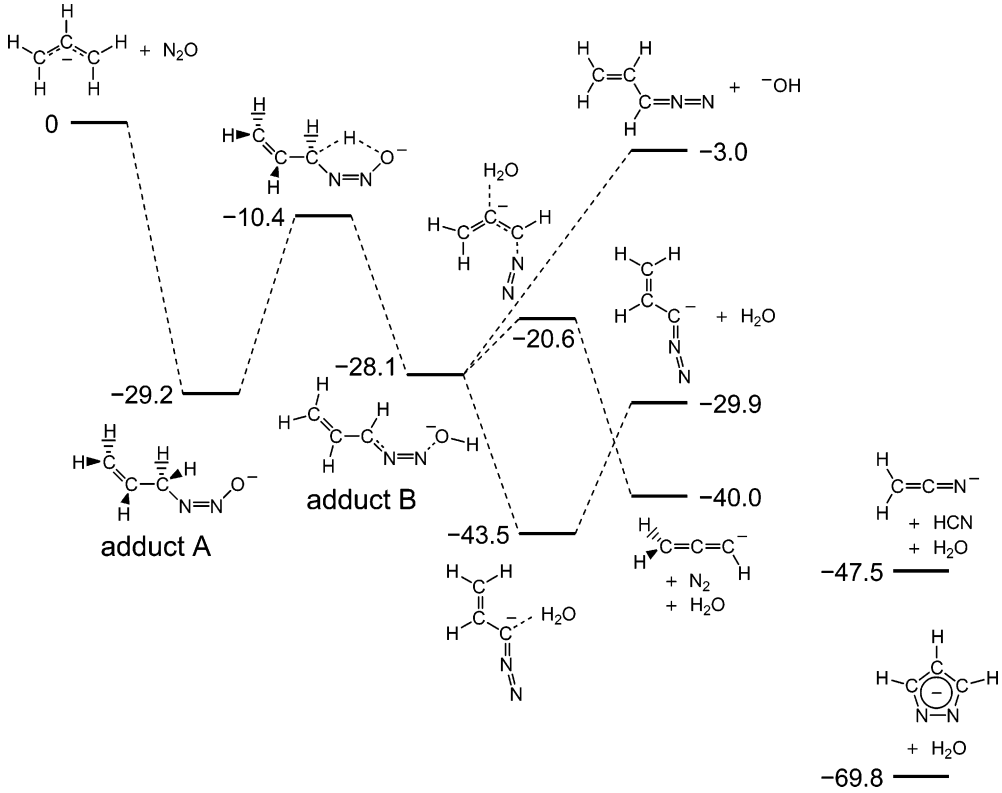

Figure 5. Energy diagram for the reaction of the allyl anion with N_2O predicted with B3LYP/6-311++G(d,p) calculations. The values represent the 298 K enthalpies of the intermediate and final product states relative to that of the reactant state in units of kcal mol^{-1}. The energy levels of the 1-pyrazolide ion and its CID products are also shown for comparison.

omethane to 1*H*-pyrazole is about 31 kcal mol^{-1} according to B3LYP/6-311++G(d,p) calculations.

Our DFT calculations suggest that the vinyldiazomethyl anion is 39.9 kcal mol^{-1} higher in energy than the 1-pyrazolide ion. In our photoelectron spectroscopic measurements, we have observed no evidence of formation of the 1-pyrazolide ion in the reaction of the allyl anion with N_2O in the flow tube. The rate coefficient of this reaction has been measured to be 1.1×10^{-11} cm^3 s^{-1}, which corresponds to a reaction efficiency of 0.012.[13] In this reaction, about 70% of the product ions are the vinyldiazomethyl anions, but HO^- (20%) and the allenyl anion (10%) have also been detected as minor products.[13] DFT calculations have been performed to survey the mechanism of the reaction of the allyl anion with N_2O, which is summarized in Figure 5.

As the allyl anion encounters N_2O, a terminal C atom of the ion bonds to the terminal N atom of N_2O. Formation of the adduct ion (adduct A) provides energy stabilization of 29.2 kcal mol^{-1}.[62] A proton attached to the C_α atom can then be transferred to the O atom. This proton transfer must overcome an energy barrier of 18.8 kcal mol^{-1}. This transition state, however, is still 10.4 kcal mol^{-1} more stable than the initial reactants. The CH bond length is 1.4449 Å while the OH bond length is 1.1977 Å at the transition state. Concomitant with the proton transfer is elongation of the NO bond. The NO bond length of adduct A is 1.2842 Å, but it becomes 1.362 Å at the transition state, and it is 1.6293 Å in the final form of the adduct ion (adduct B). Thus, adduct B has the character of HO^- bonded to the terminal N atom of vinyldiazomethane. This proton-transfer process is almost thermoneutral.

As HO^- dissociates from adduct B, it can abstract the proton from the C_α atom, the most acidic proton of vinyldiazomethane. The resulting vinyldiazomethyl anion complexed with H_2O lies 43.5 kcal mol^{-1} below the initial reactants.[63] Because of the large exothermicity, adduct B probably encounters little energy barrier along this reaction pathway. Dissociation of the complex leads to the final products, which is the major reaction pathway with an overall exothermicity of 29.9 kcal mol^{-1}. Alternatively, proton abstraction can take place at the C_β atom. The energy of the complex of the 1-diazomethylvinyl anion with H_2O is 22.9 kcal mol^{-1} below the initial reactants and only 5.3 kcal mol^{-1} above adduct B.[63] In the isolated 1-diazomethylvinyl anion, N_2 can dissociate easily because the energy barrier for the N_2 dissociation is only 2.3 kcal mol^{-1}.[64] The transition state energy shown in Figure 5 is estimated by adding the energy barrier for N_2 elimination from the isolated anion to the energy of H_2O complexation with the 1-diazomethylvinyl anion. Therefore, when the β proton is abstracted within the complex, it leads to formation of the allenyl anion, N_2, and H_2O. The overall exothermicity of this reaction path is 40.0 kcal mol^{-1}. A similar mechanism is likely to operate for N_2 elimination in the reaction of the allyl anion derived from cycloheptene with N_2O.[12] The other reaction path observed experimentally is most probably simple dissociation of HO^- from adduct B. The exothermicity of this reaction path is only 3.0 kcal mol^{-1}.

The reaction scheme illustrated in Figure 5 rationalizes the experimental findings. The inefficiency of the reaction can result from the proton-transfer process following the formation of adduct A. The branching ratio is determined by the acidity of the reaction intermediate, vinyldiazomethane. Thus, the vinyldiazomethyl anion is the major product ion, even though formation of the allenyl anion is much more exothermic overall. There is no reasonable reaction pathway available for cyclic product ion formation. Cyclization of vinyldiazomethane within the ion−molecule complex is unlikely because of the large energy barrier mentioned above. If deprotonation occurred at the terminal C atom of vinyldiazomethane, then cyclization to form the 1-pyrazolide ion would be an almost barrierless 1,5-

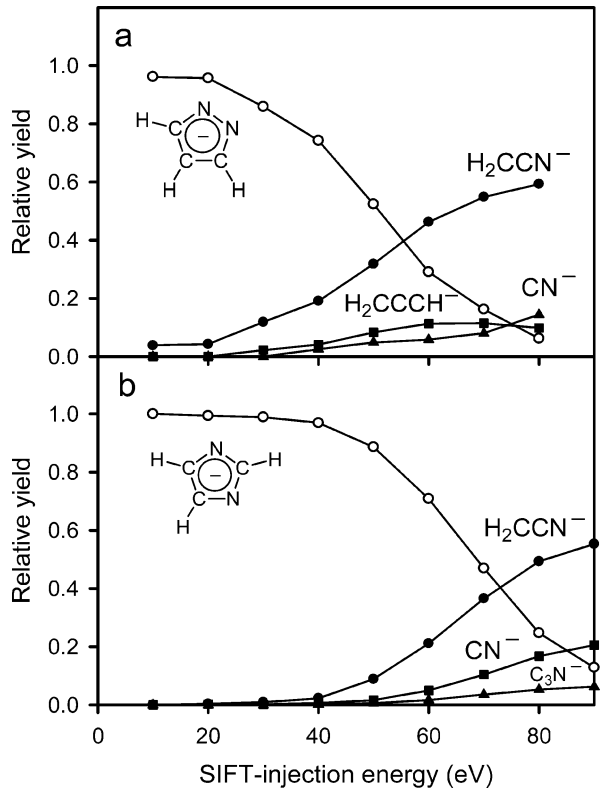

Figure 6. Relative yields of the ions produced from collision-induced dissociation of the 1-pyrazolide ion (a) and 1-imidazolide ion (b) as a function of SIFT injection energy.

electrocyclization.[59] However, proton abstraction by HO^- from the terminal C atom is about 6 kcal mol^{-1} endothermic, so reaction along this pathway is unlikely. It should be noted that 1,5-electrocyclization to form the 1-pyrazolide ion has been reported for the reaction of the diazomethyl anion with acrolein.[65]

We have performed CID measurements for the structural isomers of the vinyldiazomethyl anion, the 1-pyrazolide and the 1-imidazolide ions, to address their stability. Figure 6 shows the results of the measurements. The major product ions for the CID of the 1-pyrazolide ions are *m*/*z* 40 ions. Minor product ions at *m*/*z* 26 and *m*/*z* 39 are also observed. It is assumed that the *m*/*z* 40 ion is the cyanomethyl anion (H_2CCN^-, path a), which is the most stable $[C_2H_2N]^-$ species. This fragmentation reaction is endothermic by 26 kcal mol^{-1}.[66]

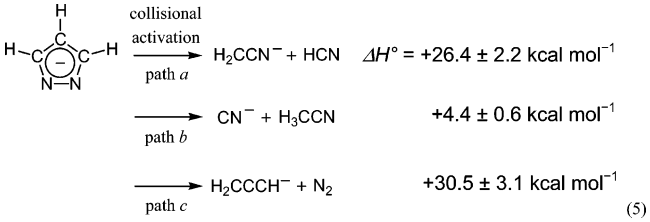

(5)

The *m*/*z* 26 ion is presumably the cyanide ion, which is formed by the most energetically favorable pathway (path b). The results suggest that the nascent fragmentation product complex is relatively short-lived such that proton-transfer equilibrium is not established within the complex. The *m*/*z* 39 ion is most probably the allenyl anion (H_2CCCH^-, path c).

CID of the 1-imidazolide ion also yields *m*/*z* 40 ions as the major product, but the 1-imidazolide ion is less susceptible to CID than the 1-pyrazolide ion under the same experimental conditions (Figure 6). The estimated CID threshold energy for the fragmentation of the 1-imidazolide ion to H_2CCN^- and HCN is 3.1 eV, compared to 2.4 eV for the corresponding fragmentation process for the 1-pyrazolide ion.[67] The minor product ions at *m*/*z* 26 and *m*/*z* 50 are assigned to be the cyanide ion and cyanoacetylide ion, respectively.

We have also investigated whether CID of the 1-pyrazolide ion leads to ring-opening without fragmentation. We used acidity bracketing to compare the reactivity of *m*/*z* 67 ions at different SIFT injection energies. The anions were injected at 20 eV (lab energy) where negligible fragmentation was observed, and at 70 eV where only a small fraction (10%) of the ions survived. Under both conditions, the *m*/*z* 67 ions exhibit essentially the same reactivity. The ions were bracketed in acidity between $(H_3C)_3CSH$ ($\Delta_{acid}G_{298} = 346.2 \pm 0.2$ kcal mol^{-1})[68−70] and CH_3SH ($\Delta_{acid}G_{298} = 351.6 \pm 0.4$ kcal mol^{-1}).[1] These results are consistent with the gas-phase acidity of pyrazole, 346.4 ± 0.3 kcal mol^{-1}.[3] The DFT calculations predict that the gas-phase acidity of vinyldiazomethane is 354.8 kcal mol^{-1}. Thus, once the ring-structure of the 1-pyrazolide ion is broken by CID, fragmentation ensues. The vinyldiazomethyl anion is 39.9 kcal mol^{-1} higher in energy than the 1-pyrazolide ion according to the DFT calculations. Therefore, isomerization of the 1-pyrazolide ion to the vinyldiazomethyl anion is 14 kcal mol^{-1} more endothermic than the fragmentation path a (reaction 5). Thus, the fragmentation is more favorable energetically.[71]

The aromaticity of five-membered, N-containing, heterocyclic compounds has been analyzed in various ways.[72,73] Schleyer and co-workers used a homodesmotic reaction to derive the aromatic stabilization energy of pyrazole as 23.7 kcal mol^{-1} with MP2(fc)/6-311+G(d,p) calculations.[74]

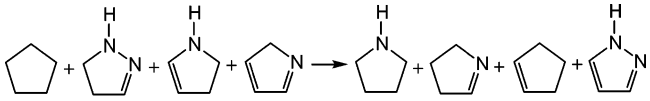
(6)

A similar reaction can be considered for the 1-pyrazolide ion.[74]

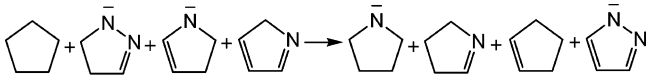
(7)

We have used B3LYP/6-311++G(d,p) calculations to estimate the aromatic stabilization energy of the 1-pyrazolide ion to be 28.9 kcal mol^{-1}. Thus, the aromaticity of the five-membered ring greatly enhances the stabilization of the cyclic form of the isomer, relative to the vinyldiazomethyl anion.

Conclusion

We have measured the 351.1 nm photoelectron spectrum of the vinyldiazomethyl anion. The ion was synthesized by the reaction of the allyl anion with N_2O in helium buffer gas in a flowing afterglow ion source. The EA of the vinyldiazomethyl radical is 1.864 ± 0.007 eV. The Franck−Condon analysis of the spectrum has been performed using the results of B3LYP/6-311++G(d,p) calculations. The simulated spectra for the *E* and *Z* conformers of the ion are distinct from each other, and the observed spectrum can be reproduced by a simulation for the *E*-vinyldiazomethyl anion. The fundamental vibrational frequencies of 185 ± 10 and 415 ± 20 cm^{-1} have been identified as the in-plane CCN and CCC bending modes of the $\tilde{X}\ ^2A''$ *E*-vinyldiazomethyl radical, respectively. The observed spectrum also displays a broad, structureless profile in the higher

eBE region. This portion of the spectrum corresponds to electron detachment producing the $\tilde{A}\ ^2A'$ state of the radical. The DFT calculations also predict that the CCN angle of the $\tilde{A}\ ^2A'$ equilibrium geometry is much larger than that of the anion geometry, which, together with the vibronic coupling with the $\tilde{X}\ ^2A''$ state, explains the broad, structureless feature of the spectrum.

Further DFT calculations have been carried out to understand the reaction mechanism of the allyl anion with N_2O, and the energetics of the vinyldiazomethyl anion has been discussed in comparison to a structural isomer, the 1-pyrazolide ion. CID measurements were also conducted for the 1-pyrazolide and 1-imidazolide ions to further explore the ion energetics. We have recently studied the reaction of HO^- with 1*H*-1,2,3-triazole, which contains three N atoms in the five-membered ring, with flowing afterglow-selected ion flow tube measurements, photoelectron imaging spectroscopic measurements, and flowing afterglow−photoelectron spectroscopic measurements. This reaction not only leads to simple deprotonation, but also induces fragmentation and ring-opening of the triazole. The reaction mechanism and ion energetics for this system will be discussed in comparison with the vinyldiazomethyl anion system, in a subsequent publication.[75]

Acknowledgment. We are pleased to acknowledge generous support from the Air Force Office of Scientific Research and the National Science Foundation.

References and Notes

(1) Gianola, A. J.; Ichino, T.; Hoenigman, R. L.; Kato, S.; Bierbaum, V. M.; Lineberger, W. C. *J. Phys. Chem. A* **2004**, *108*, 10326−10335.
(2) Gianola, A. J.; Ichino, T.; Hoenigman, R. L.; Kato, S.; Bierbaum, V. M.; Lineberger, W. C. *J. Phys. Chem. A* **2005**, *109*, 11504−11514.
(3) Gianola, A. J.; Ichino, T.; Kato, S.; Bierbaum, V. M.; Lineberger, W. C. *J. Phys. Chem. A* **2006**, *110*, 8457−8466.
(4) Klapotke, T. M. *Angew. Chem., Int. Ed.* **1999**, *38*, 2536−2538.
(5) Nguyen, M. T. *Coord. Chem. Rev.* **2003**, *244*, 93−113.
(6) Kwon, O.; McKee, M. L. Polynitrogens as promising high-energy density materials: computational design. In *Energetic Materials, Part 1: Decomposition, Crystal and Molecular Properties*; Politzer, P., Murray, J. S., Eds.; Elsevier: Amsterdam, 2003; pp 405−420.
(7) Brinck, T.; Bittererova, M.; Ostmark, H. Electronic structure calculations as a tool in the quest for experimental verification of N_4. In *Energetic Materials, Part 1: Decomposition, Crystal and Molecular Properties*; Politzer, P., Murray, J. S., Eds.; Elsevier: Amsterdam, 2003; pp 421−439.
(8) Fau, S.; Bartlett, R. J. Changing the properties of N_5^+ and N_5^- by substitution. In *Energetic Materals, Part 1: Decomposition, Crystal and Molecular Properties*; Politzer, P., Murray, J. S., Eds.; Elsevier: Amsterdam, 2003; pp 441−455.
(9) Singh, R. P.; Verma, R. D.; Meshri, D. T.; Shreeve, J. M. *Angew. Chem., Int. Ed.* **2006**, *45*, 3584−3601.
(10) Samartzis, P. C.; Wodtke, A. M. *Int. Rev. Phys. Chem.* **2006**, *25*, 527−552.
(11) Bierbaum, V. M.; DePuy, C. H.; Shapiro, R. H. *J. Am. Chem. Soc.* **1977**, *99*, 5800−5802.
(12) Kass, S. R.; Filley, J.; Van Doren, J. M.; DePuy, C. H. *J. Am. Chem. Soc.* **1986**, *108*, 2849−2852.
(13) O'Hair, R. A. J.; Gronert, S.; DePuy, C. H. *Eur. Mass Spectrom.* **1995**, *1*, 429−436.
(14) DePuy, C. H. *Org. Mass Spectrom.* **1985**, *20*, 556−559.
(15) Ervin, K. M.; Lineberger, W. C. Photoelectron Spectroscopy of Negative Ions. In *Advances in Gas Phase Ion Chemistry*; Adams, N. G., Babcock, L. M., Eds.; JAI Press: Greenwich, 1992; Vol. 1, pp 121−166.
(16) Leopold, D. G.; Murray, K. K.; Stevens Miller, A. E.; Lineberger, W. C. *J. Chem. Phys.* **1985**, *83*, 4849−4865.
(17) Ervin, K. M.; Ho, J.; Lineberger, W. C. *J. Chem. Phys.* **1989**, *91*, 5974−5992.
(18) Wenthold, P. G.; Polak, M. L.; Lineberger, W. C. *J. Phys. Chem.* **1996**, *100*, 6920−6926.
(19) Andersen, T.; Haugen, H. K.; Hotop, H. *J. Phys. Chem. Ref. Data* **1999**, *28*, 1511−1533.
(20) Rienstra-Kiracofe, J. C.; Tschumper, G. S.; Schaefer, H. F.; Nandi, S.; Ellison, G. B. *Chem. Rev.* **2002**, *102*, 231−282.
(21) Moore, C. E. *Atomic Energy Levels*; US GPO Circular No. 467, US GPO: Washington, DC, 1952.
(22) Cooper, J.; Zare, R. N. *J. Chem. Phys.* **1968**, *48*, 942−943.
(23) Van Doren, J. M.; Barlow, S. E.; DePuy, C. H.; Bierbaum, V. M. *Int. J. Mass Spectrom. Ion Processes* **1987**, *81*, 85−100.
(24) Bierbaum, V. M. Flow Tubes. In *Encyclopedia of Mass Spectrometry*; Gross, M. L., Caprioli, R., Eds.; Elsevier: Amsterdam, 2003; Vol. 1, Theory and Ion Chemistry, pp 276−292.
(25) Paulino, J. A.; Squires, R. R. *J. Am. Chem. Soc.* **1991**, *113*, 5573−5580.
(26) Becke, A. D. *J. Chem. Phys.* **1993**, *98*, 5648−5652.
(27) Lee, C. T.; Yang, W. T.; Parr, R. G. *Phys. Rev. B* **1988**, *37*, 785−789.
(28) Krishnan, R.; Binkley, J. S.; Seeger, R.; Pople, J. A. *J. Chem. Phys.* **1980**, *72*, 650−654.
(29) Frisch, M. J. et al. Gaussian 03, Revision B.05; Gaussian, Inc.: Pittsburgh, PA, 2003.
(30) Clifford, E. P.; Wenthold, P. G.; Lineberger, W. C.; Petersson, G. A.; Broadus, K. M.; Kass, S. R.; Kato, S.; DePuy, C. H.; Bierbaum, V. M.; Ellison, G. B. *J. Phys. Chem. A* **1998**, *102*, 7100−7112.
(31) Ervin, K. M. *PESCAL, Fortran program*; University of Nevada, Reno: Reno, 2003.
(32) Ervin, K. M.; Ramond, T. M.; Davico, G. E.; Schwartz, R. L.; Casey, S. M.; Lineberger, W. C. *J. Phys. Chem. A* **2001**, *105*, 10822−10831.
(33) Ho, J.; Ervin, K. M.; Lineberger, W. C. *J. Chem. Phys.* **1990**, *93*, 6987−7002.
(34) Calvi, R. M. D.; Andrews, D. H.; Lineberger, W. C. *Chem. Phys. Lett.* **2007**, *442*, 12−16.
(35) Köppel, H.; Domcke, W.; Cederbaum, L. S. *Adv. Chem. Phys.* **1984**, *57*, 59−246.
(36) Trofimov, A. B.; Köppel, H.; Schirmer, J. *J. Chem. Phys.* **1998**, *109*, 1025−1040.
(37) Selby, T. M.; Clarkson, J. R.; Mitchell, D.; Fitzpatrick, J. A. J.; Lee, H. D.; Pratt, D. W.; Zwier, T. S. *J. Phys. Chem. A* **2005**, *109*, 4484−4496.
(38) Chen, P. Photoelectron spectroscopy of reactive intermediates. In *Unimolecular and Bimolecular Reaction Dynamics*; Ng, C. Y., Baer, T., Powis, I., Eds.; John Wiley & Sons: New York, 1994.
(39) Rizzo, T. R.; Park, Y. D.; Peteanu, L.; Levy, D. H. *J. Chem. Phys.* **1985**, *83*, 4819−4820.
(40) Park, Y. D.; Rizzo, T. R.; Peteanu, L. A.; Levy, D. H. *J. Chem. Phys.* **1986**, *84*, 6539−6549.
(41) Felker, P. M. *J. Phys. Chem.* **1992**, *96*, 7844−7857.
(42) Carney, J. R.; Zwier, T. S. *J. Phys. Chem. A* **2000**, *104*, 8677−8688.
(43) Yi, J. T.; Robertson, E. G.; Pratt, D. W. *Phys. Chem. Chem. Phys.* **2002**, *4*, 5244−5248.
(44) Reese, J. A.; Nguyen, T. V.; Korter, T. M.; Pratt, D. W. *J. Am. Chem. Soc.* **2004**, *126*, 11387−11392.
(45) Williams, S.; Harding, L. B.; Stanton, J. F.; Weisshaar, J. C. *J. Phys. Chem. A* **2000**, *104*, 9906−9913.
(46) Dian, B. C.; Clarkson, J. R.; Zwier, T. S. *Science* **2004**, *303*, 1169−1173.
(47) Zwier, T. S. *J. Phys. Chem. A* **2006**, *110*, 4133−4150.
(48) Ho, Y. H.; Squires, R. R. *J. Am. Chem. Soc.* **1992**, *114*, 10961−10963.
(49) Artau, A.; Ho, Y.; Kenttamaa, H.; Squires, R. R. *J. Am. Chem. Soc.* **1999**, *121*, 7130−7137.
(50) Adeuya, A.; Artau, A.; Kenttamaa, H. I.; Squires, R. R. *J. Phys. Chem. A* **2004**, *108*, 7379−7385.
(51) Karty, J. M.; Janaway, G. A.; Brauman, J. I. *J. Am. Chem. Soc.* **2002**, *124*, 5213−5221.
(52) Chou, P. K.; Kass, S. R. *J. Am. Chem. Soc.* **1991**, *113*, 4357−4359.
(53) Romer, B. C.; Brauman, J. I. *J. Am. Chem. Soc.* **1997**, *119*, 2054−2055.
(54) Alconcel, L. S.; Deyerl, H. J.; Continetti, R. E. *J. Am. Chem. Soc.* **2001**, *123*, 12675−12681.
(55) McAllister, M. A.; Tidwell, T. T. *J. Am. Chem. Soc.* **1992**, *114*, 6553−6555.
(56) McAllister, M. A.; Tidwell, T. T. *J. Org. Chem.* **1994**, *59*, 4506−4515.
(57) The stabilization energy for the neutral system, reaction 3, is calculated to be 2.1 kcal mol^{-1} at the B3LYP/6−311++G(d,p) level.
(58) Taylor, E. C.; Turchi, I. J. *Chem. Rev.* **1979**, *79*, 181−231.
(59) Huisgen, R. *Angew. Chem., Int. Ed. Engl.* **1980**, *19*, 947−973.
(60) Labbe, G.; Mathys, G. *J. Org. Chem.* **1974**, *39*, 1778−1780.
(61) Fabian, W. M. F.; Bakulev, V. A.; Kappe, C. O. *J. Org. Chem.* **1998**, *63*, 5801−5805.
(62) The B3LYP/6-311++G(d,p) calculations show that when the allyl anion attacks the central N atom of N_2O, the resultant adduct formation is

only 4.7 kcal mol^{-1} exothermic. Thus, this adduct ion is not considered further. Also, see ref 13 and Barlow, S. E.; Bierbaum, V. M. *J. Chem. Phys.* **1990**, *92*, 3442 for the discussion of the site of N_2O reaction with ions.

(63) The B3LYP/6-311++G(d,p) energy optimization has been performed under C_s symmetry for the H_2O complex. A low imaginary frequency has been found in the harmonic frequency analysis at the stationary point with respect to hindered rotation around the OH bond. Thus, the potential energy minimum is located at C_1 symmetry, but energy lowering from the C_s to C_1 geometry is 0.1 kcal mol^{-1} or less in magnitude. The reported value is that for the C_s symmetry.

(64) We have sought a transition state for N_2 elimination from the 1-diazomethylvinyl anion under C_s symmetry. Two imaginary frequencies have been found at the stationary point. One is associated with an in-plane CN stretching mode which must directly represent the N_2 dissociation coordinate. The other is an out-of-plane mode which guides the C_3H_3 ion fragment into the optimum geometry of the allenyl anion. Thus, the reported value, which is for this C_s saddle point, should represent an upper bound for the actual transition state.

(65) DePuy, C. H.; Van Doren, J. M.; Gronert, S.; Kass, S. R.; Motell, E. L.; Ellison, G. B.; Bierbaum, V. M. *J. Org. Chem.* **1989**, *54*, 1846−1850.

(66) The reaction enthalpies for the CID processes were derived from the standard enthalpies of formation and the deprotonation enthalpies of the relevant species available in NIST Standard Reference Database Number 69, June 2005 Release.

(67) The 1-imidazolide ion is more stable than the 1-pyrazolide ion by 15.0 ± 0.8 kcal mol^{-1}, which is derived from the standard enthalpies of formation of imidazole (31.8 ± 0.2 kcal mol^{-1}) and pyrazole (42.9 ± 0.2 kcal mol^{-1}) and deprotonation enthalpies of imidazole (349.7 ± 0.5 kcal mol^{-1}, ref 2) and pyrazole (353.6 ± 0.4 kcal mol^{-1}, ref 3). The standard enthalpies of formation are from Jimenez, P.; Roux, M. V.; Turrion, C.; Gomis, F. *J. Chem. Thermodyn.* **1987**, *19*, 985−992.

(68) Bartmess, J. E.; Scott, J. A.; McIver, R. T., Jr. *J. Am. Chem. Soc.* **1979**, *101*, 6046−6056.

(69) Shiell, R. C.; Hu, X. K.; Hu, Q. J.; Hepburn, J. W. *J. Phys. Chem. A.* **2000**, *104*, 4339−4342.

(70) Ervin, K. M.; DeTuro, V. F. *J. Phys. Chem. A.* **2002**, *106*, 9947−9956.

(71) Both fragmentation to the cyanomethyl anion and hydrogen cyanide and isomerization to the vinyldiazomethyl anion require H migration.

(72) Cyranski, M. K. *Chem. Rev.* **2005**, *105*, 3773−3811.

(73) Chen, Z. F.; Wannere, C. S.; Corminboeuf, C.; Puchta, R.; Schleyer, P. v. R. *Chem. Rev.* **2005**, *105*, 3842−3888.

(74) Cyranski, M. K.; Krygowski, T. M.; Katritzky, A. R.; Schleyer, P. v. R. *J. Org. Chem.* **2002**, *67*, 1333−1338.

(75) Ichino, T.; Andrews, D. H.; Rathbone, G. J.; Misaizu, F.; Calvi, R. M. D.; Wren, S. W.; Kato, S.; Bierbaum, V. M.; Lineberger, W. C. *J. Phys. Chem. A*, submitted for publication.